Analysis and Modeling of the Transient Thermal Behavior of Automotive Turbochargers

Richard D. Burke
Department of Mechanical Engineering,
University of Bath,
Bath BA2 7AY, UK
e-mail: R.D.Burke@bath.ac.uk

Turbochargers are a key technology to deliver fuel consumption reductions on future internal combustion engines. However, the current industry standard modeling approaches assume the turbine and compressor operate under adiabatic conditions. Although some state of the art modeling approaches have been presented for simulating the thermal behavior, these have focused on thermally stable conditions. In this work, an instrumented turbocharger was operated on a 2.2 liter diesel engine and in parallel a one-dimensional lumped capacity thermal model was developed. For the first time this paper presents analysis of experimental and modeling results under dynamic engine operating conditions. Engine speed and load conditions were varied to induce thermal transients with turbine inlet temperatures ranging from 200 to 800 °C; warm-up behavior from 25 °C ambient was also studied. Following a model tuning process based on steady operating conditions, the model was used to predict turbine and compressor gas outlet temperatures, doing so with an RMSE of 8.4 and 7.1 °C, respectively. On the turbine side, peak heat losses from the exhaust gases were observed to be up to double those observed under thermally stable conditions due to the heat accumulation in the structure. During warm-up, the model simplifications did not allow for accurate modeling of the compressor, however on the turbine side gas temperature prediction errors were reduced from 150 to around 40 °C. The main benefits from the present modeling approach appear to be in turbine outlet temperature prediction, however modeling improvements are identified for future work. [DOI: 10.1115/1.4027290]

Keywords: heat transfer, turbocharger, transient, model, experiment, engine

1 Introduction

Turbochargers are an important component for achieving significant internal combustion engine improvements through downsizing. Demonstrator engines have shown up to 35% vehicle fuel consumption reduction through reduced engine capacity and boosting.

During engine development the focus on performance simulations is very much toward peak torque, steady operation. In contrast, in service and on future homologation drive cycles, the behavior at lower loads and under significantly dynamic operating conditions will be more important. Under these conditions heat transfer in turbochargers becomes significant as do the thermal inertias of its components; for cold starting applications the gas temperature leaving the turbine is important for after-treatment specification.

There is therefore a need to be able to predict the thermal behavior of the turbocharger in engine simulations during the development phase. This paper aims to study this behavior under transient conditions and develop a simple mathematical model for use in conjunction with one-dimensional engine performance calculations.

2 Background

Engine performance simulation using one-dimensional (1D) gas dynamics codes conventionally ignore heat transfer effects. The turbine and compressor behavior is based on measured data from steady flow experiments undertaken by the turbocharger manufacturer. These *maps* are supplied under corrected temperature and pressure conditions, and no indication of actual test conditions is retained. These steady flow experiments include a degree of heat transfer, however on-engine conditions are considerably different due to flow conditions and installation effects; these result in different levels of heat transfer on-engine compared to gas stand and consequently simulation inaccuracies.

While studies have shown limited influence of thermal behavior on the swallowing capacity of the devices (i.e., the relationship between pressure ratio, rotational speed, and air flow), there are significant impacts on the apparent efficiency of the device [1,2]. The effects are expressed both as an influence on isentropic efficiency or on the temperature after the compression/expansion processes. As mentioned previously, the heat transfer effects are mixed with the work transfer, however it is important to bear in mind that the changes in temperature are both due to work and heat transfer.

A number of authors have studied heat transfer in turbochargers under steady flow conditions. The majority of studies focus on the influence of turbine inlet temperature on the apparent efficiency of the compressor.

Cormorais et al. [2] undertook investigations on a steady flow gas stand with the turbocharger insulated to avoid external heat transfers. By varying the gas temperature at the inlet to the turbine between 50 and 500 °C they discovered a drop in apparent compressor efficiency of 10–15 percentage points. Shaaban [3] undertook similar experiments without insulating the turbocharger, varying turbine inlet temperature between 30 and 700 °C and observed smaller influence on compressor apparent efficiency. Serrano et al. [1] also conducted steady flow experiments at 270–580 °C which are less extreme than the two previous studies. These authors showed only small influence on compressor efficiency and even a slight improvement in efficiency. The authors concluded that this was due to heat transfer from the compressed gases to the compressor casing when the compression was strong

Contributed by the Combustion and Fuels Committee of ASME for publication in the Journal of Engineering for Gas Turbines and Power. Manuscript received February 18, 2014; final manuscript received February 25, 2014; published online May 2, 2014. Editor: David Wisler.

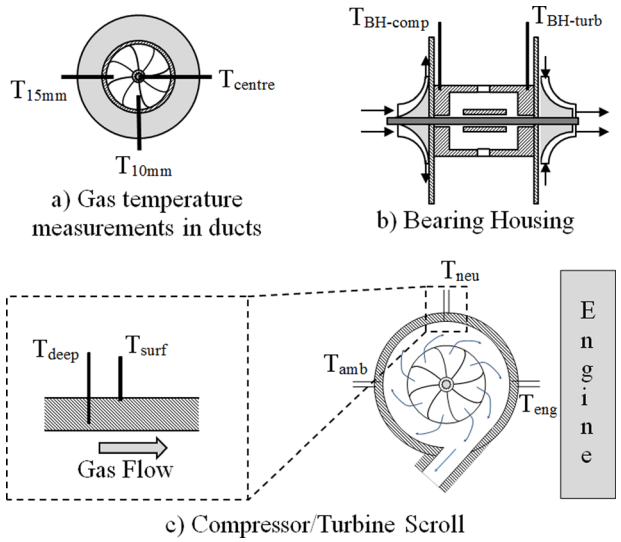

Fig. 1 Turbocharger thermal instrumentation

enough to heat the gases sufficiently. Heat losses on the turbine side are primarily transferred to oil and ambient rather than the compressor when thermal insulation is not installed.

Baines et al. [4] studied thermal effects under both forced and free external convection cooling and at turbine inlet temperatures between 87 and 257 °C. Their work suggested that internal heat transfers to the lubricating oil was up to 3 times larger than to ambient. This was considerably lower than the results from Shaaban [3] who found 70% of heat transfer on the turbine side to flow to ambient; however at such low turbine inlet temperatures there will be smaller thermal gradients to ambient. In fact, the work by Baines measured heat transfer in the turbine only up to 700 W, which is significantly lower than the 2.7 kW measured by Aghaali and Angstrom [5] from engine test data. Romagnoli and Martinez-Botas [6] studied heat transfer effects on a turbocharger installed on an engine running under constant engine speed and brake torque conditions. They observed that installation in proximity to the engine and exhaust manifold influence heat transfer and measured outer surface temperature differences of up to 60 °C from sides facing the engine to those facing ambient.

A number of mathematical modeling approaches have been proposed to account for thermal behavior of turbochargers. The majority of these approaches are based on the assumption that the compression and expansion processes remain adiabatic, and that heat transfer occurs before or after the rotor. This can be justified by the difference in heat transfer area which is smaller in the rotor than in the housings. Shaaban [3] proposes an analytical solution to the heat transfer between turbine and compressor assuming a one-dimensional heat flow. Although this approach accounts for oil losses and can account for thermal effects under stable conditions, the lack of thermal masses makes the model unsuitable for transient conditions. Olmeda et al. [7] proposed a one-dimensional lumped model based on the electrical analogy. The turbocharger is simplified into a small number of thermal capacities which are linked together via conduction, convection, and radiation. This model was composed of four fluid nodes (turbine gas, compressor gas, cooling water, and lubricating oil) and five metal nodes (turbine housing, compressor housing, and three sections of bearing housing). Further work by the same authors describe a specific experimental procedure on a dedicated test facility to determine the various parameters of the model [8]. Romagnoli and Martinez-Botas [6] developed a more elaborate one-dimensional model based on the same principles, but using an increased number of thermal nodes from a simplified three-dimensional geometry of the device. Bohn [9] implemented a three-dimensional conjugate flow and heat transfer simulation. Initially a full turbocharger model was considered but as computational times were excessive the study was limited to only the compressor side and boundary conditions were determined experimentally from thermal imaging. The results demonstrated a relatively uniform compressor housing temperature and by analyzing heat flows along the gas path through the compression, showed the reversal of heat transfer if the heating by compression is strong enough. Although arguably the most complete modeling approach, the three-dimensional calculation remain impractical in conjunction with engine performance simulation due to the long running times.

From the review of relevant work in the field of turbocharger heat transfer it may be concluded that

- although ignored in engine simulations, heat transfer in the turbine and compressor can represent a significant proportion of energy transfer in the turbocharger.
- only a small proportion of heat from the turbine is transferred to the compressor unless unusual conditions are in place (insulated turbocharger, high turbine inlet temperature, and low compressor flows).
- heat transfer in the compressor can occur in both directions depending on the level of heating through compression which can increase the gas temperatures above the casing temperatures.
- 1D thermal network seem the most promising for engine simulation codes and can account for the accumulation of thermal energy under transient conditions.
- none of the studies published in the literature measure or model heat transfer on-engine, operating under dynamic conditions; conditions which are more representative of real world operation.

In the present study, an instrumented turbocharger was installed on an engine facility operating under transient conditions. A one-dimensional heat transfer model was developed in parallel and the transient performance predictions were assessed.

3 Experimental Apparatus

An automotive turbocharger was instrumented and installed on a 2.2 liter diesel engine, operated on a dynamic ac dynamometer facility. The turbocharger was cooled and lubricated by engine oil provided from the engine.

In total 40 thermocouples were installed to measure a range of fluid and metal temperatures: at each of the four compressor and turbine gas inlets, three thermocouples were installed to measure gas temperature at different penetrations into the flow. Metal temperatures were measured at three locations around the turbine scroll and three locations around the compressor scroll. At each location, two sensors were installed, one close to the gas side wall, the other close to the outer surface; thus giving a temperature gradient. Two metal temperatures were also measured on the bearing housing, one near the turbine housing the other near the compressor housing. Details of the thermocouple installation are given in Fig. 1.

All temperatures were measured using 1.5 mm mineral insulted thermocouples; the accuracy of the tip temperatures is quoted within 2–6 °C. It is also of interest to estimate the accuracy of the temperature measurements over dynamic events where the thermal mass of the thermocouple will induce a dynamic aspect to the measurement. A simple analysis is undertaken assuming that the heat transfer to the thermocouple occurs only through convection. The temperature change of the thermocouple tip can then be calculated according to Eq. (1),

$$m_{\mathrm{TC}} C_{p\_\mathrm{TC}} \frac{dT_{\mathrm{TC}}}{dt} = h_c A_{\mathrm{TC}} \left(T_g - T_{\mathrm{TC}}\right) \tag{1}$$

Assuming the thermocouple is initially in thermal equilibrium with the gas stream at a temperature $T_{\mathrm{gas},0}$, the thermocouple

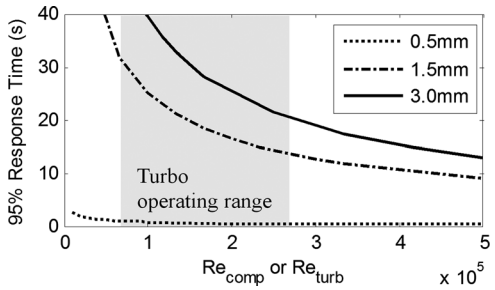

Fig. 2 95% response time of 0.5, 1.5, and 3 mm diameter thermocouple in air flow at 200 °C as a function of Reynolds number

Table 1 Steady state engine operating points in terms of brake torque and engine speed

	Engine speed (rpm)				
Torque (N m)	1000	1500	2000	2500	3000
50	X	X	X	X	X
100	X		X		
150	X				X
200		X		X	
300		X	X	X	

temperature following a step change in gas temperature ΔT_{gas} is given by Eq. (2),

$$T_{\text{TC}}(t) = T_{g,0} + \Delta T_g\left(1 - e^{-t/\tau}\right) \quad \text{where } \tau = \frac{m_{\text{TC}} C_{p\_\text{TC}}}{h_{\text{conv}} A_{\text{TC}}} \tag{2}$$

The time constant τ in Eq. (2) is indicative of the response time of the thermocouple and a time of 3τ corresponds to a response of 95%. For a given thermocouple size, fluid composition, and fluid temperature this value is a function of Reynolds number and is plotted for air at 200 °C for 0.5, 1.5, and 3 mm diameter thermocouples in Fig. 2. Also shown is the operating range of the turbocharger turbine and compressor from this study. This shows that for 1.5 mm thermocouples used in this work, the response time will vary from 10 to 30 s. Moving to smaller diameter thermocouples would significantly increase the response times, however in the authors experience also leads to excessive sensor failures.

Oil flow to the turbocharger was measured using an OvalGear Positive displacement flow meter with measurement accuracy of ±1%. Fresh air flow into the engine was measured using an ABB Sensyflow hot film sensor with an expected error of less than 1%. Flow through the turbine was assumed to be equal to the sum of air flow and fuel flow, with fuel flow measured from a Gravimetric fuel balance. Pressures were measured using remote Druck PTX type sensor with an accuracy of 0.25%.

A series of stationary and transient experiments were conducted operating the engine under a range of speed and brake torque conditions. Each experiment described above was repeated three times to assess the repeatability of the measurements and test control as well as increase confidence in the measured results. For stationary tests, following a 20 min warm-up at 1500 rpm/100 N m, the engine was thermally soaked at each operating points for a period of 7 min before data logging was taken as a mean over a 100 s period. The list of operating points is given in Table 1 and these were run to minimize the thermal offsets between consecutive points, starting from highest and moving to the lowest engine power.

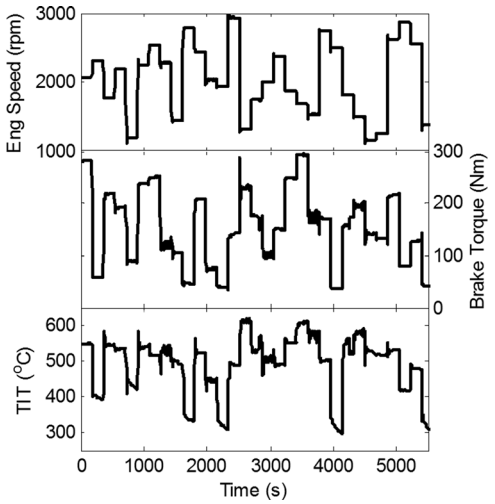

Fig. 3 Engine speed, brake torque, and turbine inlet temperature (TIT) for dynamic experiments

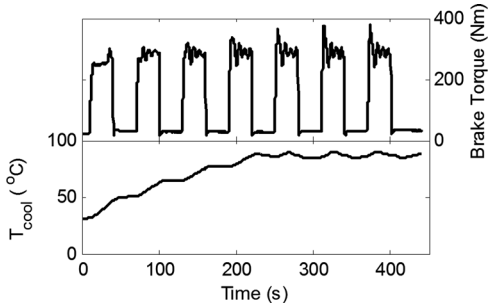

Fig. 4 Brake torque and engine coolant temperature for ambient start experiment

A number of transient experiments were also conducted where the engine was operated at a series of speed/load conditions. The hold time at any condition was limited to 3 min thus not allowing the system to settle thermally before moving to the next condition. The speed and brake torque traces for this experiment are shown in Fig. 3; the almost step changes in speed and engine torque were in fact ramped over 3 s periods. Also shown is the induced variation in turbine inlet temperature.

A further transient experiment was conducted to assess the system behavior and model performance during warm-up from ambient start temperature (25 °C). Directly after engine firing, the engine speed was held constant at 1250 rpm, while engine load was switched between 30 N m and full load sequentially with a period of 60 s; the engine brake torque and coolant temperature are shown in Fig. 4. As the engine warms up the maximum brake torque that can be achieved increases mainly as a result of reducing frictional losses.

4 Model Structure

A simplified mathematical model of the turbocharger was built to predict thermal behavior of the system. The model assumes that the compression and expansion processes are adiabatic and heat transfer between the working fluids and the structure occur both before and after these processes. The compressor and turbine housings are considered as two masses of constant temperature, linked by thermal conduction. The compressor and turbine wheels are mounted on a fixed rotor; an outline of the model structure is shown in Fig. 5. Heat losses by conduction to adjacent components such as exhaust manifold, exhaust pipe, and catalytic convertor are ignored. The use of only two lumped masses compared

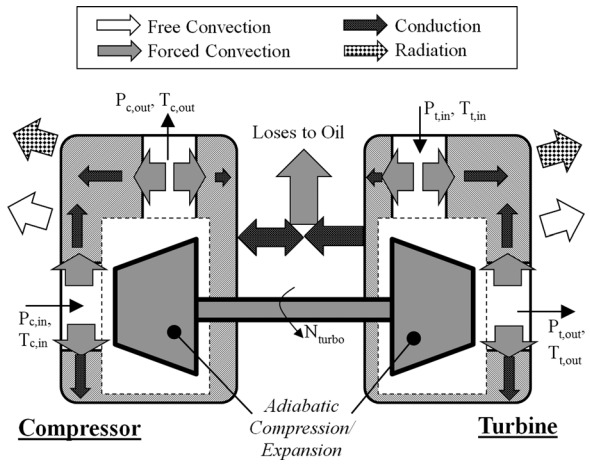

Fig. 5 Diagram of mode structure

Table 2 Constants for convective heat transfer correlations

Correlation	a_1	a_2	a_3	a_4
Seider–Tate	0.027	0.8	1/3	0.14
UoB exhaust	1×10^{-6}	2.02	1/3	0.14
UoB intake	0.004	1.13	1/3	0.14

to the other authors that used additional nodes to represent the central bearing housing is justified in this study because of the simple empirical modeling of heat transfer to oil.

The compression and expansion processes are considered adiabatic and the relationships between pressure ratio, mass flow, rotational speed, and isentropic efficiency (and VGT position for turbine) are described by operating maps measured on steady flow facilities. Air flow is described as a function of pressure ratio and speed while isentropic efficiency is described as a function of pressure ratio and mass flow, and VGT rack position for the turbine (Eqs. (3)–(6)). The operating speed of the turbocharger is determined by a power balance based on turbine power extraction and compressor power usage (Eq. (7)). Due to the measurement method of turbine isentropic efficiency, the frictional losses in the journal bearing are included in the turbine map

$$\dot{m}_{\text{comp}} = f\left(PR_{\text{comp}}, N_{\text{turbo}}\right) \tag{3}$$

$$\dot{m}_{\text{turb}} = f\left(PR_{\text{turb}}, N_{\text{turbo}}, VGT\right) \tag{4}$$

$$\eta_{\text{comp}} = f\left(PR_{\text{comp}}, \dot{m}_{\text{comp}}\right) \tag{5}$$

$$\eta_{\text{turb}} = f\left(PR_{\text{turb}}, \dot{m}_{\text{turb}}, VGT\right) \tag{6}$$

$$\frac{dN}{dt} = \frac{60}{2\pi I_{\text{turbo}}}\left(\tau_{\text{turb}} - \tau_{\text{comp}}\right) \tag{7}$$

Convective heat transfer from the working gases (fresh intake air and combustion exhaust gases) was modeled using Newton's law of cooling (Eq. (8)). The area was taken to be the total internal area of gas flow paths, determined from geometrical data. This is split proportionally into two areas: before and after compression/expansion. For a typical turbocharger layout, the ratio for both turbine and compressor is roughly 85% on the high pressure side and 15% on the low pressure side. The convective heat transfer coefficients were initially determined using the Seider–Tate correlation (Eq. (9)). It should be noted that in the turbine a highly pulsating flow exists, however in this approach a mean Reynolds number was used, based on engine cycle average. As will be seen later, this resulted in significant underestimation of heat transfer and therefore a custom heat transfer correlation was derived based on stationary experiments. The coefficients for derived heat transfer correlations for compressor and turbine side are shown along with the original Seider–Tate coefficients in Table 2

$$Q_c = h_{\text{in}} A_{\text{in}}\left(T_g - T_w\right) \tag{8}$$

$$\text{Nu} = a_1 \text{Re}^{a_2} \text{Pr}^{a_3}\left(\frac{\mu_{\text{bulk}}}{\mu_{\text{skin}}}\right)^{a_4} \tag{9}$$

Conduction through the turbine and compressor housing was modeled using Fourier's law assuming one-dimensional heat flow (Eq. (10)). The thickness is assumed uniform for each of the four sections of the device, while the area is again determined using the split as above for convective heat transfer

$$Q_{c,\text{in}} = \frac{A_{\text{in}} k}{dx}\left(T_{\text{in}} - T_{\text{out}}\right) \tag{10}$$

Losses to ambient are split into two parts: radiation and convection. Radiation heat transfer is determined using Eq. (11). The outer area was the total outer area of the turbine or compressor housing, determined from the part geometry; unlike internal convection, only a single transfer was considered as it was assumed that the casing temperature was uniform. The emissivity of the turbine and compressor housings was based on that of cast iron and aluminum, respectively,

$$Q_{\text{rad}} = A_{\text{out}} \varepsilon \sigma\left(T_{\text{out}}^4 - T_{\text{amb}}^4\right) \tag{11}$$

Convection losses were modeled using the method described by Eriksson [10] (Eq. (12)). Cell ventilation was achieved through large intake and exhaust air ducts in the ceiling of the test cell. Although they displace large amounts of air, the air movement near the turbocharger was expected to be small; therefore a free convection correlation was used.

$$h_{c,\text{ext}} = 1.25\left(T_{\text{wall}} - T_{\text{amb}}\right)^{1/3} \tag{12}$$

Conduction in the bearing housing was again assumed to be one dimensional and losses to ambient from the bearing housing were ignored in this simple model. The bearing housing was assumed to be a simple cylinder. The thermal conductivity of the bearing housing was that of cast iron; the contact resistance with the compressor housing was ignored.

Heat transfer to oil Q_{oil} was modeled using an empirical relationship based on measured values from stationary experiments and described as a function of engine power. Heat generation due to friction was ignored in this model.

To allow the simulation of transient events, the model must capture the accumulation and release of heat from the two thermal masses representing the compressor and turbine housings. These are defined by Eqs. (13) and (14); for simulation of steady state experiments, the masses were reduced to approximately 1/100th their true value to reduce computation times, however for transient simulations the actual masses were used.

$$dT_{\text{comp}} = \frac{Q_{c,\text{in},b} + Q_{c,\text{in},a} + Q_{k,\text{BH}} - Q_{\text{oil}} - Q_{\text{rad}} - Q_{c,\text{out}}}{c_{p,\text{comp}} m_{\text{comp}}} \tag{13}$$

$$dT_{\text{turb}} = \frac{Q_{c,\text{in},b} + Q_{c,\text{in},a} - Q_{k,\text{BH}} - Q_{\text{rad}} - Q_{c,\text{out}}}{c_{p,\text{turb}} m_{\text{turb}}} \tag{14}$$

The initial model was configured using parameters as defined above and based on correlation from the literature. However, a model tuning phase was also conducted using the stationary data measured in this work. It was assumed that all of the modeling error would be grouped into the modeling of convective heat

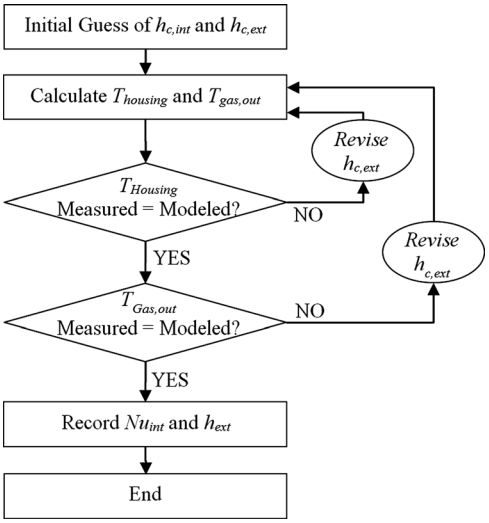

Fig. 6 Convection model identification approach for each test point

transfer both on the inner and outer surfaces. This was deemed reasonable as on the inner surface, an average Reynolds number was used to describe highly pulsating flows. On the external surface, no data were available relating to the air motion in the proximity of the turbocharger and although no spot cooling fans were used, there could be channeling or general air ventilation due to the engine shape. The measurements of gas temperatures at the compressor and turbine exit were used in combination with the measured housing temperatures to calculate new convective correlations according to Fig. 6. This process was used to derive measured Nusselt numbers for the internal convection and correction factors for external convection.

5 Results

The results section will be split into three sections: the first will cover analysis of steady state experiments, the second will present the dynamic step based experiments, and the third will show warm-up behavior.

5.1 Steady State Experiments. Initially the temperature distribution around the turbocharger scroll is considered: temperatures from selected operating points are given in Table 3 (temperature locations refer to those described in Fig. 1). Considering first the compressor, the temperature drops through the wall (difference deep, surf) range from 0 to 26 °C with higher temperature gradients at higher engine operating powers, where compressed gases would be hotter through higher compression. These results are similar to those published by Romagnoli and Martinez-Botas [6] for a similar engine. However, temperature differences around the scroll (from engine to ambient side) are less than 14 °C in all cases which is considerably less than the previous authors who observed up to 64 °C variation. These differences may be explained by the layout of the engine: Romagnoli and Martinez-Botas [6] used a front wheel drive configuration where the turbocharger is mounted above the exhaust manifold, EGR cooler, and exhaust pipe. In contrast, in this work a rear wheel drive installation is used with the turbocharger mounted below the exhaust manifold and away from the exhaust pipe; a heat shield is also installed between the compressor housing and the manifold.

On the turbine side differences around the circumference of the scroll are comparable to those published by Romagnoli and Martinez-Botas (29–71 °C compared to 23–64 °C). However, measured temperature gradients through the scroll wall are considerably larger. Notably, the external surface temperatures appear lower than would be expected from the literature. One explanation may be poor thermal contact between the thermocouples and the surface, meaning the measurement is actually affected by the local air temperature, no longer giving a true metal temperature. Clearly this is unacceptable for further heat transfer analysis and in subsequent sections only the inner *deep* temperatures were considered.

For the 14 steady state operating points measured on the test facility, three models were used to calculate the compressor and turbine outlet gas and wall temperatures:

(1) model with no heat transfer (map based)
(2) nontuned heat transfer model
(3) tuned heat transfer model using the method described in Fig. 6

The predicted temperatures are plotted against measured values in Fig. 7. For both compressor and turbine gas outlet temperatures the prediction is improved through the inclusion of the heat

Table 3 Selected metal temperatures from compressor and turbine scroll (all temperatures in °C)

	Compressor			Turbine		
T (°C)	Deep	Surf	ΔT_{wall}	Deep	Surf	ΔT_{wall}
Engine speed: 1000 rpm, engine torque: 50 N m						
Eng	50	50	0	218	156	62
Neu	50	45	5	214	156	58
Amb	51	47	4	189	124	62
$\Delta T_{eng\text{-}amb}$	1	5		29	32	
Engine speed: 1000 rpm, engine torque: 150 N m						
Eng	64	64	0	363	265	98
Neu	65	56	9	358	254	104
Amb	66	59	7	315	204	111
$\Delta T_{eng\text{-}amb}$	2	8		48	61	
Engine speed: 1500 rpm, engine torque: 300 N m						
Eng	129	117	12	525	374	151
Neu	132	106	26	520	356	164
Amb	134	120	14	454	307	147
$\Delta T_{eng\text{-}amb}$	5	14		71	67	
Engine speed: 3000 rpm, engine torque: 150 N m						
Eng	130	114	16	420	263	157
Neu	134	108	26	418	278	140
Amb	134	121	13	363	242	121
$\Delta T_{eng\text{-}amb}$	4	13		57	36	

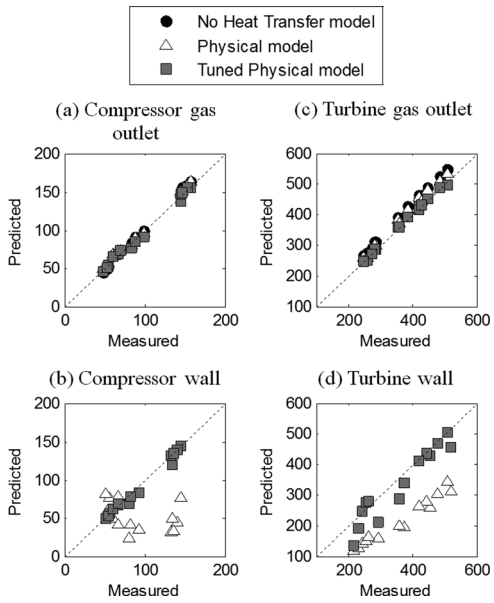

Fig. 7 Compressor and turbine gas outlet and wall temperature predictions for no heat transfer mode, physical model, and tuned physical model compared to measured values

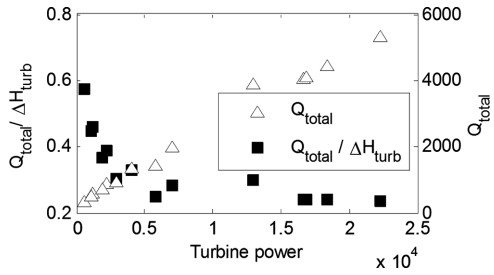

Fig. 8 Absolute turbine heat transfer and fraction of total enthalpy change

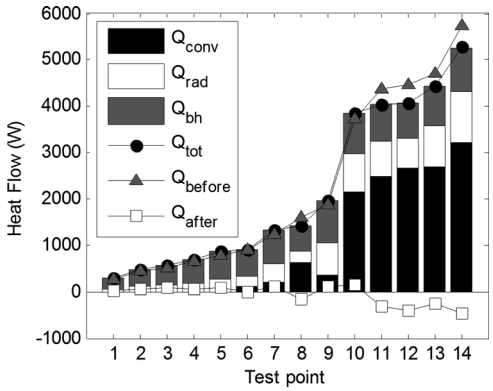

Fig. 9 Turbine heat flow breakdown including convection before and after expansion (Q_{before} and Q_{after}), conduction to bearing housing (Q_{BH}), and convection and radiation to ambient (Q_{conv} and Q_{rad})

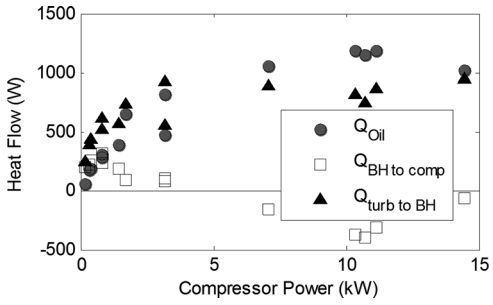

Fig. 10 Heat flow in bearing housing from turbine housing ($Q_{turb\ to\ BH}$), to oil (Q_{oil}) and from bearing housing to compressor housing ($Q_{BH\ to\ comp}$); negative values signify reversal of heat flow

transfer model. On the compressor side, the effect of the heat transfer model on outlet gas temperature prediction is moderate, reducing the mean absolute error from 4 to 3 °C. On the turbine side, without a heat transfer model, the outlet gas temperature is systematically overestimated by an average of 32 °C; the inclusion of the heat transfer model reduced this to ±4 °C. The nontuned physical model offers only a partial benefit in terms of prediction accuracy and the housing wall temperatures give an insight into this: there is a considerable underestimate of turbine wall heat transfer while the prediction of compressor wall is very poor. For the turbine side, this is most probably a result of the assumption of a mean Reynolds number when in fact the flow is highly pulsating. Results on the compressor side will also be affected by the underestimate of heat transfer on the turbine side. The tuned model uses the structure of the Seider–Tate correlation, with fitted coefficients as described in Table 2; this model allows wall prediction for compressor and turbine with mean absolute deviation of 4 and 33 °C, respectively.

The heat transfer model predicts heat flows in the turbocharger. For the turbine side, the heat flow from the exhaust gases to the housing are split into two portions: that transferred before the expansion (Q_b) and that occurring after (Q_a). Figure 8 shows the total heat transfer (Eq. (15)) in absolute terms and relative to total enthalpy change in the turbine (Eq. (16)), both with respect to turbine shaft power (estimated from compressor enthalpy rise). This shows that over the operating points considered in this work, the heat transferred in the turbine is roughly proportional to the work transfer. The heat transfer represents between 20% and 60% of total enthalpy change, representing a larger proportion at lower shaft work. The breakdown of heat transfer before and after expansion is given by the lines in Fig. 9. This shows that the majority of heat is transferred before the expansion process owing to the larger area and higher temperature of the gases at the higher pressure. In fact, at the highest turbine shaft powers, the model suggests that the expansions process would cool the exhaust gases below the mean housing temperature resulting in heat transfers of up to 300 W reheating the gas.

$$Q_{\text{total}} = Q_b + Q_a \tag{15}$$

$$\Delta H_{\text{turb}} = \dot{m}_{\text{turb}} C_p \Delta T_{\text{turb}} \tag{16}$$

The breakdown of heat transfer from the turbine housing is shown in the stacked bars of Fig. 9. At higher turbine powers this shows that the majority of heat is lost to ambient via convection and radiation to the surroundings (77%–82% in cases 10–14). The proportions are considerably higher than those observed by Baines et al. [4] who operated the turbocharger at much lower temperatures, but of similar magnitudes to those published by Shaaban and Seume [11]. At lower loads when the turbine temperature is lower, the majority of heat tends to flow towards the bearing housing where it is dissipated in the oil or transferred to the compressor housing (71%–83% in cases 1–5).

The bearing housing energy balance is shown in Fig. 10 and details heat flows from the turbine housing, to oil and to the compressor housing (negative values indicate reversal of heat flow); each are shown as a function of compressor power, based on total enthalpy rise through the compressor. At low compressor powers the heat transfer from the turbine housing is larger than the cooling by engine oil resulting in a net positive heat flow to the

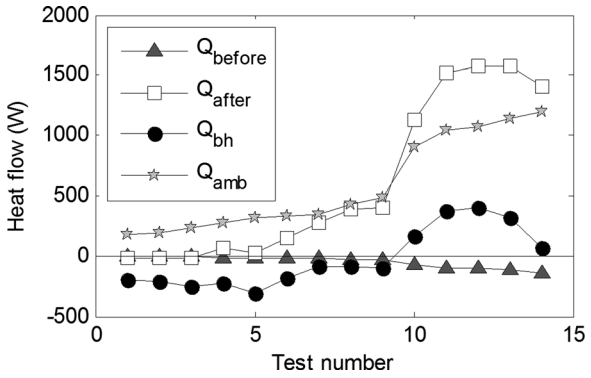

Fig. 11 Compressor heat flow breakdown showing convection before and after compression (Q_{before} and Q_{after}, positive means from working fluid), conduction to beaing housing (Q_{BH}, positive means to bearing housing) and to ambient (Q_{amb}, positive to ambient)

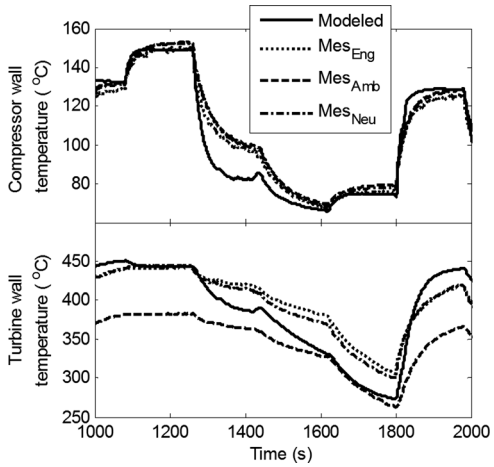

Fig. 12 Measured and predicted compressor and turbine wall temperatures during transient experiment (eng, amb, and neu correspond to locations in Fig. 1)

compressor housing. For compressor powers above 5 kW, such is the increase in temperature due to compression, heat flows from the compressor housing to the bearing housing (negative values for $Q_{BH\ to\ comp}$ in Fig. 10). This is consistent with other published work on nonthermally insulated turbochargers, operating under high load conditions.

The energy balance on the compressor side is illustrated in Fig. 11: this shows the heat transfer between the working fluid and housing before and after compression, the losses to ambient and heat transfer with the bearing housing. Heat is always transferred from the housing to the cold gases entering the device before the compression; this rises with increasing compressor power from 4 to 150 W. Only at very low powers (below 0.5 kW) is further heat transferred to the compressed gases; above this limit heat transfers of up to 1.5 kW are observed to the compressor housing. Under low compressor power conditions, up to 300 W of heat is transferred to the compressor housing from the bearing housing, this provides the heat transferred to the intake gases, but over 80% of this heat is transferred to ambient via convection and radiation (test cases 1–3). As compressor power increases, ambient losses increase as they are composed of heat from the bearing housing and heat from the compressed gases (test cases 4–9). As heat from the compressed gases increases further, heat flows with the bearing housing reverse, effectively resulting in oil cooling the compressor housing.

The analysis of heat flows under steady engine operating conditions has resulted in a tuned heat transfer model providing adequate predictions of metal and gas temperatures in the turbocharger. The validated model will be used for transient predictions without further modification (other than the application of true housing mass calculated from three-dimensional geometry). Analysis of heat flows predicted by the model are in line with findings published by other authors; notably the proportion of exhaust heat flowing to ambient and the cooling of compressor housing by oil at high compressor powers.

Table 4 Fit statistics for turbocharger model for gas and wall temperatures for models with and without heat transfer effects

	No heat transfer model			With heat transfer model		
	RMSE	nRMSE	R^2	RMSE	nRMSE	R^2
$T_{wall\ Comp}$	N/A	N/A	N/A	8.9 °C	9.8%	0.88
$T_{wall\ turb}$	N/A	N/A	N/A	20.6 °C	10.5%	0.80
$T_{gas\ out\ comp}$	9.8 °C	8.8%	0.89	7.1 °C	6.5%	0.95
$T_{gas\ out\ turb}$	35.8 °C	14.5%	0.90	8.4 °C	3.4%	0.98

5.2 Dynamic Experiments. The results from the dynamic experiments need to bear in mind the analysis of temperature measurement dynamics described in Sec. 3: the 95% response time of the thermocouples installed in the gas stream was estimated to be between 10 and 30 s.

Figure 12 shows the evolution of compressor and turbine wall temperatures, both measured and predicted by the heat transfer model over a 16 min period of the transient experiment. For both the turbine and compressor housing temperature measurements, the transient response approximated to a first order system response and the settling time can be calculated through statistical fitting of a first order system response: these are estimated at 150 and 240 s for compressor and turbine housings, respectively. As the thermocouple response for these temperatures depends on conduction rather than convection, the measurement system dynamics are of less a concern than for gas temperatures. In both cases, the prediction underestimates the dynamic effects suggesting the actual thermal masses are greater than those measured and used in this work. Over the complete experiment, the following model fit statistics are calculated: Root mean square error (RMSE), normalized RMSE (nRMSE), and coefficient of determination (R^2); these are described in Eqs. (17) to (19) and given in Table 4.

$$R^2 = 1 - \frac{\sum(\hat{y} - \bar{y})^2}{\sum(y - \bar{y})^2} \tag{17}$$

$$\text{RMSE} = \sqrt{\frac{\sum(\hat{y} - y)^2}{n}} \tag{18}$$

$$\text{nRMSE} = \frac{\text{RMSE}}{\bar{y}} \tag{19}$$

Measured and simulated gas temperatures are shown in Fig. 13 for the same 16 min period; predicted values from both simulations with and without heat transfer model are presented. This figure gives an insight into the dynamics and it can be seen that for some step changes these prevail for the complete duration of the 3 min holding times, notably on the turbine side. In these cases the thermal response is clearly significantly larger than the thermocouple response calculated previously. However, in other cases the dynamics are of similar order of magnitude to the thermocouple response and in this case it will not be possible to separate the two effects. The model prediction over the complete experiment is described in Fig. 14 and summarized in Table 4. On the compressor side, the inclusion of the heat transfer model improves the prediction only slightly, with the RMSE reducing from 9.8 to 7.1 °C. On the turbine side the improvement is significantly larger with the RMSE reducing from 35.8 to 8.4 °C.

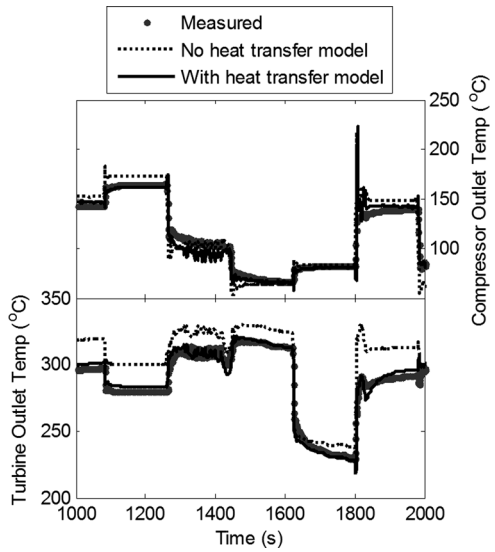

Fig. 13 Measured and modeled compressor and turbine outlet temperatures over short period of dynamic step experiment

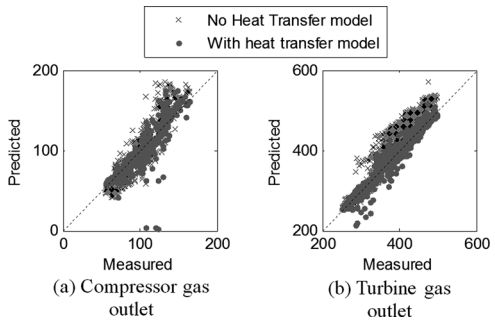

Fig. 14 Predicted compressor and turbine outlet gas temperatures over dynamic step cycle with and without heat transfer model

Figure 15 shows the energy flows during a section of the transient experiment. The boundary conditions in the first two frames show that the particular maneuver driving the thermal behavior results from an increase in turbine inlet temperature from around 300 to 480 °C. Very rapidly this causes an increase in turbocharger shaft speed from 110 to 160 krpm. This corresponds to a situation immediately after the step changes where the compressor and turbine housing will be colder than those experienced under steady state conditions. The compressor heat flows (shown in frame 3) show that over a 30 s period following the change in conditions, a much higher heat flow from the compressed gas to the housing is measured. As heat is stored in the compressor housing and the structure warms up, this heat flow reduces to a stable level. At the same time, heat losses to ambient gradually increase to 1 kW after a 40 s period.

On the turbine side (heat flows shown in frame 4), increased heat flows of up to 6.6 kW are measured into the structure; after around 100 s this has reduced to around 0.6 kW.

To generalize the results shown in Fig. 15, some signal analysis was conducted of each of 30 step responses. The basic quantities are illustrated in the first and forth frame of Fig. 15:

- The magnitude of exhaust gas temperature step T_{step} is the difference between the exhaust gas temperature just prior to the step and that 3 min after the step.
- The peak heat transfer from the exhaust gases Q_{peak} is defined as the maximum (or minimum depending on the shape of the response) heat flow during the first 60 s following the step change in operating conditions.

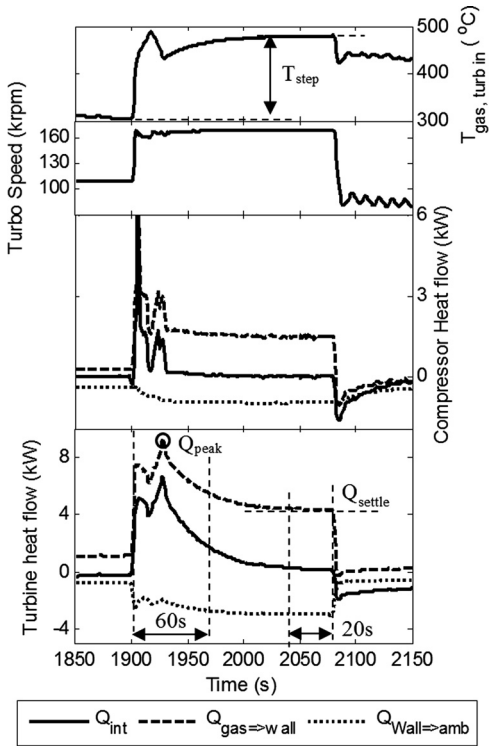

Fig. 15 Section of dynamic experiment showing turbine inlet temperature (top frame), shaft speed (second frame), and compressor and turbine heat flows (third and bottom frame). Heat flow show transfer from gas to wall ($Q_{gas=>wall}$), accumulation in structure (Q_{int}), and external transfer from wall to ambient ($Q_{wall=>amb}$).

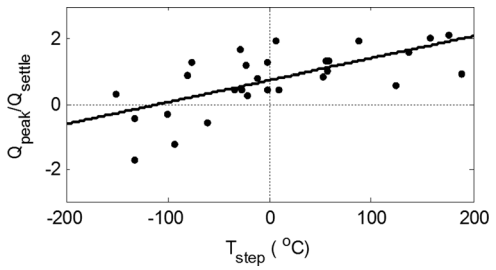

Fig. 16 Ratio of dynamic to steady heat flow from exhaust gases to turbine housing as a function of step change in exhaust gas temperature

- The steady heat flow Q_{settle} is the mean heat flow over the period 160–180 s after the step change, corresponding to the last 20 s before the next step change.

Using these quantities, the ratio of dynamic heat flow to steady heat flow is plotted against T_{step} in Fig. 16. This shows a relationship between the magnitude of temperature change and the onset of heat flows: the larger the change in turbine inlet temperature, the larger the initial heat transfer compared to the settling value. When assessing the results it is important to bear in mind that Q_{settle} was always a positive value. The majority of points are located in the upper half of the graph. Those points located in the lower left quadrant correspond to situations where the peak heat flow is reversed (i.e., from the casing to the exhaust gases) following relatively large reductions in exhaust gas temperature flowing into a relatively hot casing. For points in the upper half, those with a Q_{peak}/Q_{settle} value of less than 1 have a lower initial heat transfer than under stable conditions and correspond mainly to points in the upper left quadrant, i.e., following smaller step reductions in

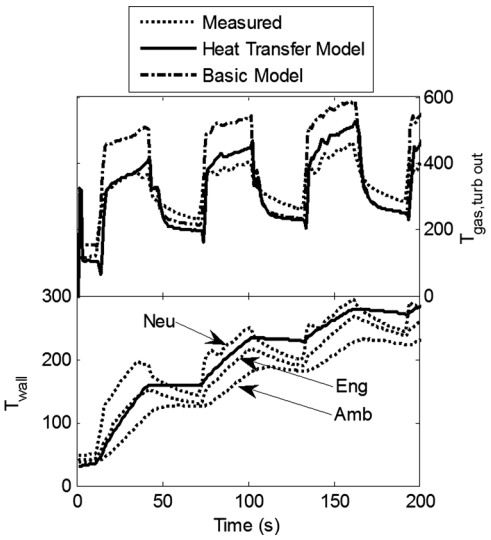

Fig. 17 Measured and predicted turbine gas outlet and turbine wall temperatures during warm-up period; amb, eng, and neu correspond to temperature locations described in Fig. 1

exhaust gas temperature. Most of the points in the upper right quadrant have Q_{peak}/Q_{settle} values greater than 1 which would be expected following an increase in exhaust gas temperature into a relatively cold turbine housing. There are no points in the lower right quadrant of the graph which would correspond to initial heat flows from the turbine casing to the exhaust gas following a step increase in exhaust gas temperature.

There are a number of points that are exceptions to these rules showing the dynamic response is not only a function of exhaust gas temperature step size but also other factors, notably changes in mass flow rate will also influence this behavior.

5.3 Ambient Start Dynamic Experiments. For the ambient start experiments, the prediction of compressor temperatures was very poor and is not presented in this paper. During warm-up, the assumption of one-dimensional heat flow may no longer be valid; equally the basic modeling of heat transfer to oil used in this work will break down. On the turbine side where temperature gradients are much larger between the exhaust gases and the ambient, the predictions are considerably better and are shown in Fig. 17. The turbine gas temperature prediction both with and without the heat transfer model is shown relative to the measured gas temperature in the upper frame. The base model significantly overpredicts the outlet temperature by up to 150 °C; this is considerably larger than the overprediction for steady state operation which was an average of 32 °C. This larger error is indicative of the larger heat losses, while the turbine casing is warming up following cold start. The inclusion of the heat transfer model significantly improves the prediction, although errors of 40 °C are still observed. This is encouraging as the model assumptions are quite compromising the cold start simulation and clearly there remains scope for further refinement. Turbine wall temperature measurements and predictions are shown in the lower frame of Fig. 17 and show good agreement.

6 Discussion

The steady flow work has given an insight into the heat flows within a turbocharger operated on a diesel engine at a range of operating conditions. These are in line with findings from other authors using similar turbocharger installation and operating conditions. The simplified modeling of heat transfer using a mean Reynolds number required some level of empirical calibration for the forced convection processes on the internal surfaces of the turbine and compressor. Similar levels of uncertainty were considered for external heat transfer.

The modeling work is based on the assumption that the compression and expansion processes are adiabatic, and that this behavior can be represented by empirical data measured from steady flow facilities. However, the measurements undertaken to produce these performance maps will also include a degree of heat transfer. By consequence, the heat transfer model calibrated in this work accounts not for the absolute heat transfer, but the difference in heat transfer between the conditions where the maps were produced and the conditions on-engine. Future work in this area should employ back to back steady flow/on-engine experiments and seek to reverse model heat transfer on steady flow measurements such as to produce a truly adiabatic map. Despite these limitations a reasonable model was achieved improving the prediction quality of exit gas temperatures from the turbocharger.

The assumptions in the modeling approach have a more significant impact under transient conditions. As only a two mass representation was adopted, the central bearing housing is not included in the model; however its thermal inertia will also contribute to transient behavior. Second, heat loss to oil was accounted for empirically using steady state measurements; under transient conditions oil temperatures and flows will be different and therefore provide an additional source of inaccuracy. For both compressor and turbine, despite underestimating dynamics of the casing temperatures, the gas temperatures were well captured; this suggests that the relationship between gas and metal temperature is of greater importance than the absolute accuracy of the metal temperature itself.

Simulation of cold start performance presented further limitations with respect to oil heat transfer. Also until temperature gradients develop, the assumption of one-dimensional heat flow will be significantly wrong. For the compressor, simulation prediction was poor, however on the turbine side where higher temperature gradients are involved and a high proportion of the heat is transferred to ambient rather than the bearing housing, predictions were better. This is promising in providing predictions for catalyst light-off.

7 Conclusions

An experimental and thermal survey of an automotive turbocharger was conducted under steady and transient engine operating conditions. The following conclusions can be drawn:

(1) With exception to the lowest flow rates, heat flow on the compressor side is predominantly from the compressed gases to the compressor housing.
(2) A simple two-mass model of the turbocharger can provide significant improvements in gas temperature prediction, reducing RMSE from 9.8 and 35.8 °C to 7.1 and 8.4 °C for compressor and turbine, respectively; this is achieved despite larger inaccuracies in housing temperature prediction.
(3) Prediction of warm-up behavior was only possible for turbine side, however this allowed exhaust gas temperature for catalyst light-off to be predicted with errors of around 40 °C, reduced from 150 °C for conventional modeling approaches.
(4) The presented modeling approach relies on empirical maps of the aerodynamic performance that are considered to be adiabatic, application of the heat transfer model to these measurements is required to derive the true adiabatic performance as heat transfer does occur even in gas stand conditions.
(5) Further work should include the refinement of temperature measurements to improve the transient response and the control of external heat transfer. Modeling improvements should provide inclusion of the central bearing housing, predictive representation of heat transfer to oil, and the consideration of instantaneous Reynolds number during pulsating flow operation.

Acknowledgment

The author would like to acknowledge the funding of the EPSRC Knowledge Transfer Account as well as Jaguar Land-Rover, Ford Motor Company, and Cummins Turbo Technologies. The work was undertaken within the Powertrain and Vehicle Research Centre at the University of Bath, UK and the contributions from the technical staff are also acknowledged.

Nomenclature

a = constant
A = area (m^2)
Cp = heat capacity (J/kg K)
h = heat transfer coefficient (W/m^2 K)
H = enthalpy (J)
I = moment of inertia (kg m^2)
k = thermal conductivity (W/mK)
m = mass (kg)
n = number of measurements
N = rotational speed (rpm)
nRMSE = normalized RMSE
Nu = Nusselt number
Pr = Prandtl number
PR = pressure ratio
Q = heat (W)
R^2 = coefficient of determination
Re = Reynolds number
RMSE = root mean square error
t = time (s)
T = temperature (K,R °C)
VGT = variable geometry position
x = distance (m)
y = measured output
$\hat{y}$ = predicted output
$\bar{y}$ = mean measured output
ε = emissivity
μ = dynamic viscosity (N s/m^2)
σ = Stefan–Boltzman constant (5.670 W/m^2 K^4)
τ = time constant, torque S, N m

Subscripts

a = after compression/expansion
amb = ambient or exterior surface
b = before compression/expansion
BH = bearing housing
c = convection
comp = compressor
cool = coolant
eng = engine side
ext = external
g = gas
in = inner surface, internal
k = conduction
neu = neutral, upper surface
out = outer surface
rad = radiation
turb = turbine
turbo = turbocharger
TC = thermocouple
w = wall

References

[1] Serrano, J. R., Guardiola, C., Dolz, V., Tiseira, A., and Cervello, C., 2007, "Experimental Study of the Turbine Inlet Gas Temperature Influence on Turbocharger Performance," SAE Paper No. 2007-01-1559.
[2] Cormerais, M., Hetet, J. F., Chesse, P., and Maiboom, A., 2006, "Heat Transfer Analysis in a Turbocharger Compressor: Modeling and Experiments," SAE Paper No. 2006-01-0023.
[3] Shaaban, S., 2004, "Experimental Investigation and Extended Simulation of Turbocharger Non-Adiabatic Performance," Ph.D. Thesis, Universität Hannover, Hannover, Germany.
[4] Baines, N., Wygant, K. D., and Dris, A., 2010, "The Analysis of Heat Transfer in Automotive Turbochargers," ASME J. Eng. Gas Turbines Power, **132**(4), p. 042301.
[5] Aghaali, H., and Angstrom, H.-E., 2012, "Improving Turbocharged Engine Simulation by Including Heat Transfer in the Turbocharger," SAE Paper No. 2012-01-0703.
[6] Romagnoli, A., and R. Martinez-Botas, 2012, "Heat Transfer Analysis in a Turbocharger Turbine: An Experimental and Computational Evaluation," Appl. Thermal Eng., **38**(3), pp. 58–77.
[7] Olmeda, P., Dolz, V., Arnau, F. J., and Reyes-Belmonte, M. A., 2013, "Determination of Heat Flows Inside Turbochargers by Means of a One Dimensional Lumped Model," J. Math. Comput. Model., **57**(7–8), pp. 1847–1852.
[8] Serrano, J. R., Olmeda, P., Paez, A., and Vidal, F., 2010, "An Experimental Procedure to Determine Heat Transfer Properties of Turbochargers," Measure. Sci. Technol., **21**(3), p. 035109.
[9] Bohn, D., Heuer, T., and Kusterer, K., 2005, "Conjugate Flow and Heat Transfer Investigation of a Turbo Charger," ASME J. Eng. Gas Turbines Power, **127**(3), pp. 663–669.
[10] Eriksson, L., 2002, "Mean Value Models for Exhaust System Temperatures," SAE Paper No. 2002-01-0374.
[11] Shaaban, S., and Seume, J. R., 2006, "Analysis of Turbocharger Non-Adiabatic Performance," Institution of Mechanical Engineers: 8th International Conference on Turbochargers and Turbocharging, London, May 17–18.